J Fluoresc (2013) 23:1173–1178
DOI 10.1007/s10895-013-1248-0

ORIGINAL PAPER

A New On-fluorescent Probe for Manganese (II) Ion

Kaku Dutta · Ramesh Ch. Deka · Diganta Kumar Das

Received: 23 January 2013 / Accepted: 17 June 2013 / Published online: 26 June 2013

Abstract A new fluorescent probe for Mn^{2+} ion, (6E)-N-((E)-1,2-diphenyl-2-(pyridin-2-ylimino)ethylidene)pyridin-2-amine (**L**), has been synthesized from benzil and 2-amino pyridine and characterized. In 1:1 (v/v) CH_3CN:H_2O (pH 4.0, universal buffer) **L** exhibits fluorescent intensity with emission peak at λ_{max} 360 nm on excitation with photons of 310 nm. Fluorescent intensity of **L** increases distinguishingly on interaction with Mn^{2+} ion compared to metal ions—Na^+, K^+, Ca^{2+}, Mg^{2+}, Ba^{2+}, Fe^{2+}, Co^{2+}, Ni^{2+}, Cu^{2+}, Zn^{2+}, Cd^{2+}, Hg^{2+}, Pb^{2+} and Ag^+ individually or all together. The enhancement in fluorescent intensity is due to snapping of photoinduced electron transfer (PET) prevailed in free L. Fluorescence and UV/visible spectral data analysis shows that binding stoichiometry between Mn^{2+} and L is 1:1 with log $\beta \approx 3.0$. Both L and its Mn^{2+} complex were optimised using density functional theory (DFT) and vibrational frequency calculations confirm that both are at local minima on the potential energy surfaces.

Keywords Manganese(II) · 2-aminopyridine · Benzil · Fluorescence sensor · Probe · Photoinduced electron transfer (PET) · DFT

Introduction

Manganese (Mn) is an essential trace nutrient in all forms of life with wide biological roles [1, 2]. Mn is also important in photosynthetic oxygen evolution [3]. Human body contains about 12 mg of Mn [1, 4]. Mn compounds are less toxic, however, exposure to manganese dusts and fumes above the ceiling value of 5 mg/m^3 even for short periods is toxic and has been linked to impaired motor skills and cognitive disorders [5–8]. Consumption of high level of Mn in drinking water is associated with increased intellectual impairment and reduced intelligence quotients in children [9]. There is report of possible link between Mn inhalation and central nervous system (CNS) toxicity in rats [10]. Mn overexposure and/or dysregulation leads to oxidative stress, mitochondrial dysfunction, glutamate-mediated excitoxicity, aggregates of protein and manganism (a rare neurological disorder) [11, 12].

Design and development of fluorescent sensors for detecting metal ions have gained significant interest due to their simplicity, high sensitivity and real-time detection [13–17]. Although, a good number of fluorescent sensors have been actualized that can detect different kinds of metal ions [18] only a few fluorescent sensors for Mn^{2+} ion have been reported till date. A novel pH-controlled recognition method for the discriminative detection of Mn^{2+} and Cu^{2+} ions via CdTe quantum dot fluorescence sensing has been developed [19]. A new approach for Mn^{2+} ion sensing by fluorescence "off-on" mode has been reported very recently based on supramolecular metal displacement method [20]. 1,2 bis-(o-aminophenoxy)ethane-N,N,N,N-tetraacetic acid (bapta) based fluorescent probe has been recently reported for Mn^{2+} [21]. A good number of commercial dyes are known to show fluorescence on interaction with Mn^{2+} but they lack selectivity particularly with respect to Ca^{2+} [22].

In this paper, we report that a new compound derived from benzil and 2-amino pyridine, (6E)-N-((E)-1,2-diphenyl-2-(pyridin-2-ylimino)ethylidene)pyridin-2-amine (L), acts as fluorescence sensor for Mn^{2+} ion in 1:1 (v:v) acetonitrile-water by switch "on" mode. This fluorescent probe is free from interferences of a good number of metal ions—Na^+, K^+, Ca^{2+}, Mg^{2+}, Ba^{2+}, Fe^{2+},

K. Dutta · D. K. Das (✉)
Department of Chemistry, Gauhati University,
Guwahati 781014, Assam, India
e-mail: digkdas@yahoo.com

R. C. Deka
Department of Chemical Sciences, Tezpur University,
Napaam, Tezpur 784 028, Assam, India

Scheme 1 Structure of the probe L (**a**) and its DFT optimised form (**b**)

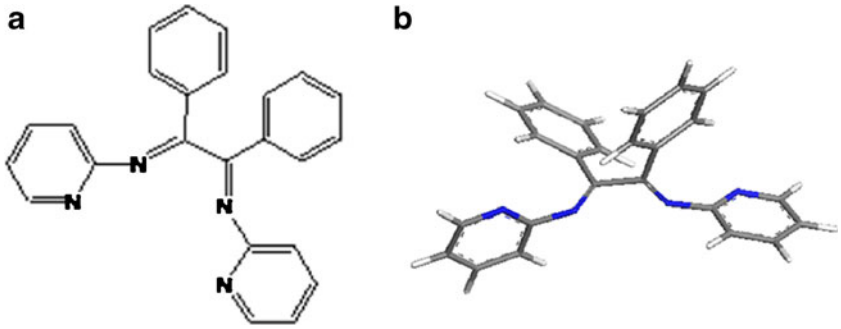

Co^{2+}, Ni^{2+}, Cu^{2+}, Zn^{2+}, Cd^{2+}, Hg^{2+}, Pb^{2+} and Ag^{+}. The binding stoichiometry and binding constant between Mn^{2+} ion and L has also been reported.

Experimental

All the chemicals and metal salts were purchased from Merck. Most of the metal salts are sulphates except lead and silver salts are nitrates while mercury and calcium slats are chlorides. The metal salts were recrystallized from water (Millipore) before use. Metal salt solutions (10^{-2} M) were prepared in 1:1 (v/v) CH_3CN:H_2O (pH 4.0, universal buffer). Fluorescent spectra were recorded in a Hitachi 2500 spectrophotometer using quartz cuvette. A 7.4×10^{-4} M solution of L in 1:1 (v:v) CH_3CN:H_2O (pH 4.0, universal buffer) was used in the experiments. UV/Visible spectra were recorded in a Shimadzu UV 1800 spectrophotometer. ^1H NMR spectra were recorded in a Bruker Ultrashield 300 spectrometer. All NMR spectra were obtained in $CDCl_3$ at room temperature and the chemical shifts are reported in δ values (ppm) relative to TMS.

In DFT calculations the initial structure of L and the Mn^{2+} ion complex were generated from the available experimental data. L and its Mn^{2+} complex were fully optimized using BLYP functional and DNP basis sets as implemented in the program DMol^3 [23]. In order to confirm the stability of the complexes we performed vibrational frequencies calculations at the optimized structure with the same level of theory.

Synthesis and Characterization of L

L (Scheme 1a) was prepared by dissolving 2.0 mmol (1.88 g) of 2-Amino pyridine and 1.0 mmol (2.10 g) of benzil in MeOH (30 mL) in a round bottom flask and stirred 12 h to get solid product. The dark greenish product obtained was filtered, washed with water, dried and recrystallized from dichloromethane (DCM). Yield: 80 %; solubility: DCM, Acetonitrile, dimethylsulfoxide.

FTIR spectrum of L (KBr pellet): 1,590 cm^{-1}, 2,742 cm^{-1} & 2,820 cm^{-1} ($\nu_{=C-H}$); 1,372 cm^{-1} & 1,250 cm^{-1} (ν_{C-N}); 905 cm^{-1} (δ_{C-H}).

^1H NMR spectra of L ($CDCl_3$, TMS, δ ppm): 7.5 (t) ppm and 7.8 (d) ppm (-CH- of benzene ring); 7.6 (d) ppm (-CH- of pyridine ring, 2 β C=N); 7.9 (s) ppm (-CH- of pyridine ring, 2 β C=N); 8.1 (s) ppm (-CH- of pyridine ring, 1 α C=N).

We have optimized the structure of L using DFT (Scheme 1b). Vibrational frequency calculations confirmed that L is at local minima on the potential energy surfaces.

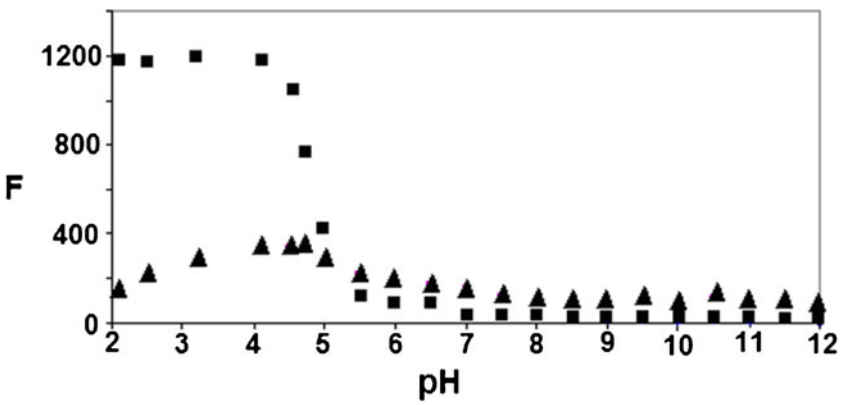

Fig. 1 Effect of pH in the range 2.0 to12.0 (universal buffer) on the fluorescent intensity of L (▲) and 1:1 concentration ratio between L and Mn^{2+} (■)

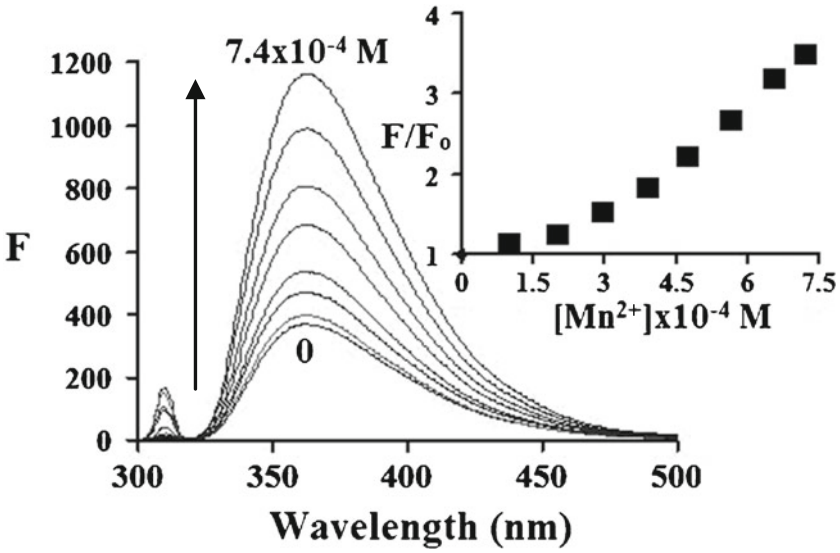

Fig. 2 Fluorescence emission spectra of L at different added concentration of Mn^{2+} ion in 1:1 (v/v) $CH_3CN:H_2O$ solution (from 0.99×10^{-4} M to 7.4×10^{-4} M) (λ_{ex}=310 nm; λ_{emi}=300–650 nm; Inset: plot of F/F_o as a function of Mn^{2+} ion concentration)

Results and Discussion

The fluorescence spectrum of L (7.4×10^{-4} M) was recorded in 1:1 (v/v) $CH_3CN:H_2O$ in the pH range 2.0–12.0 (universal buffer) at room temperature using 310 nm photons for excitation (Fig. 1). L exhibited an emission band at 300 nm to 650 nm with λ_{max} at 360 nm. The fluorescence emission intensity was found to increase moderately from pH 2.0 to pH 4.0, then remained almost unchanged till pH 5.2 and thereafter showed a gradual decrease till pH 12.0. All our further experiments have been performed at pH 4.2.

Addition of Mn^{2+} ion into the solution induced a gradual enhancement in intensity of the fluorescence spectrum of L till the concentration ratio between L and Mn^{2+} ion became 1:1 (Fig. 2). The final enhancement in fluorescence intensity was *ca*. 3.5 times of the original intensity. Inset of Fig. 2 shows the plot of F/Fo as a function of Mn^{2+} ion concentration, where F is the fluorescence intensity at a given concentration of Mn^{2+} ion and F_o is the intensity at zero concentration of Mn^{2+} ion. The plot of F/F_o value versus concentration of Mn^{2+} ion is linear in the concentration range 2×10^{-4} M to 7.2×10^{-4} M (R^2=0.991).

Figure 1 also shows the effect of pH on the fluorescent intensity of the Mn^{2+} ion saturated solution of L. The fluorescent intensity was in "on" state from pH 2.0 to pH 4.2 and started to decrease, attained "off" state at pH 5.5 and remained "off" thereafter. This experiment shows that 4.2 is the optimum pH value for highest fluorescent intensity of $L:Mn^{2+}$ interaction.

Fluorescence spectra of L (10^{-4} M) was also recorded at different added concentration (from 10^{-4} M to 10^{-3} M) of metal ions—Na^+, K^+, Ca^{2+}, Mg^{2+}, Ba^{2+}, Fe^{2+}, Co^{2+}, Ni^{2+}, Cu^{2+}, Zn^{2+}, Cd^{2+}, Hg^{2+}, Pb^{2+} and Ag^+. Figure 3 is the bar diagram profile comparing the effect of various metal ions, at 1.0 mM concentration, on the F/F_o value of L. The metal ions K^+, Co^{2+}, Zn^{2+}, Pb^{2+} and Ag^+ were found to quench the fluorescence intensity of L to a small extent while Fe^{2+} and Hg^{2+} ions quenched the fluorescence intensity of L considerably. Little enhancement in

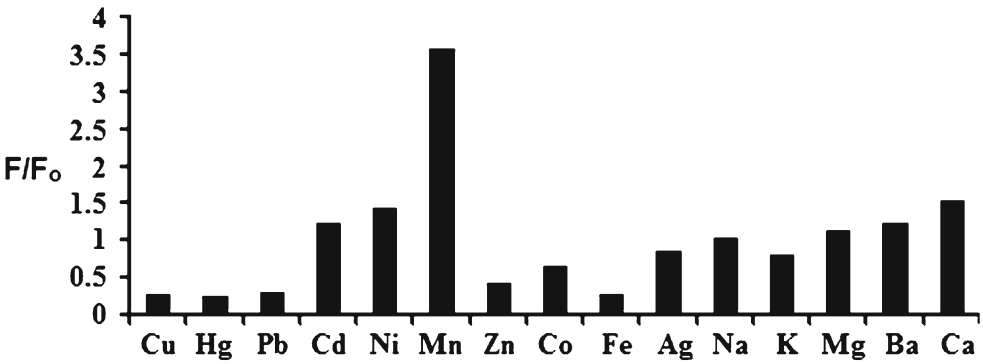

Fig. 3 Bar diagram showing the effect of 1 equivalent of different metal ions (7.4×10^{-4} M) on the fluorescence intensity of L in 1:1 (v/v) $CH_3CN:H_2O$

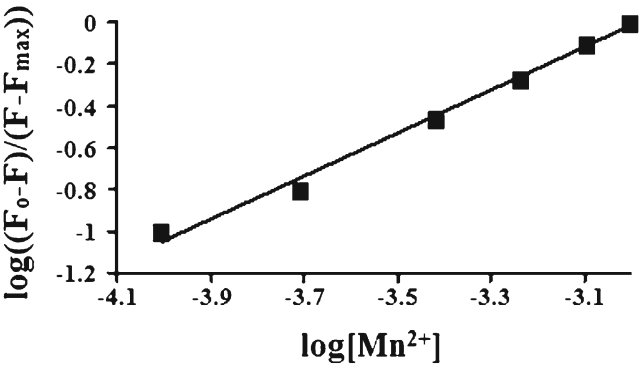

Fig. 4 Plot of $\log((F_o-F)/(F-F_{max}))$ versus $\log[Mn^{2+}]$ for titration of L against Mn^{2+} in 1:1 (v/v) $CH_3CN:H_2O$, slope 1.03 indicates 1:1 complexation between Mn^{2+} and L

fluorescence intensity was observed when L interacted with metal ions—Na^+, Mg^{2+}, Ba^{2+}, Ca^{2+}, Ni^{2+}, Cu^{2+} and Cd^{2+}.

We investigated the combined interfering effect of all the other metal ions on the fluorescence sensing of Mn^{2+} ion by L. For this purpose we prepared three solution mixtures where concentration of each metal ion was 10^{-5} M, 10^{-4} M and 10^{-3} M together with 10^{-4} M L. Fluorescent intensity of these three solutions were recorded in absence of Mn^{2+} ion and in presence of 10^{-4} M Mn^{2+} ion. Presence of Mn^{2+} ion induced an enhancement in fluorescence intensity by 3.42, 3.37 and 3.32 times respectively to the intensity when Mn^{2+} ion was absent. These values are quite close to 3.5 time enhancement in fluorescent intensity induced by Mn^{2+} ion when no other metal ions were present. This experimental result has confirmed that L is highly selective for Mn^{2+} ion in presence of other metal ions together.

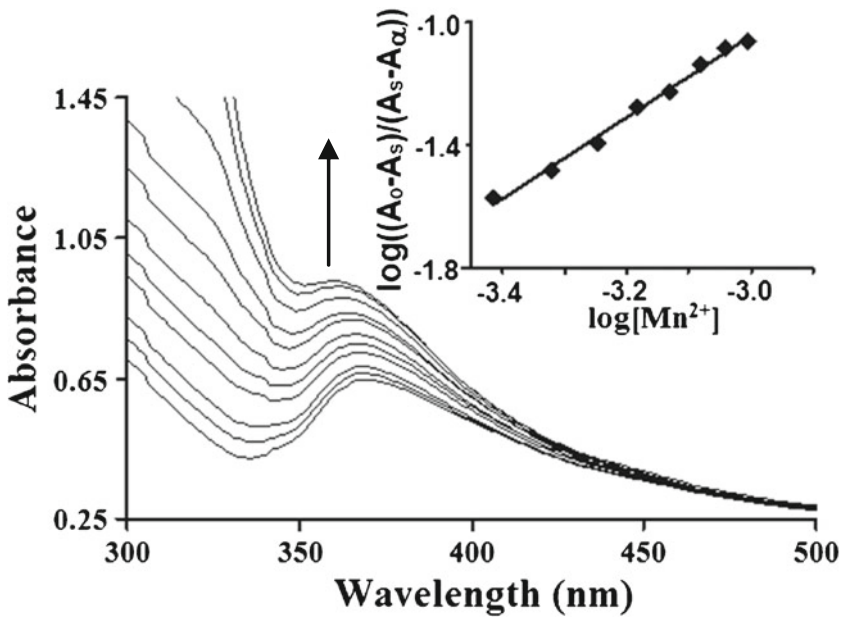

Fig. 5 The absorbtion spectrum of L in 1:1 (v/v) $CH_3CN:H_2O$ solution at different added concentration of Mn^{2+} (from 0.99×10^{-4} M to 7.4×10^{-4} M) (Inset: plot of $\log((A_o-A_s/A_s-A_\alpha))$ as a function of Mn^{2+} ion concentration, slope 1.11 indicates 1:1 complexation between Mn^{2+} and L

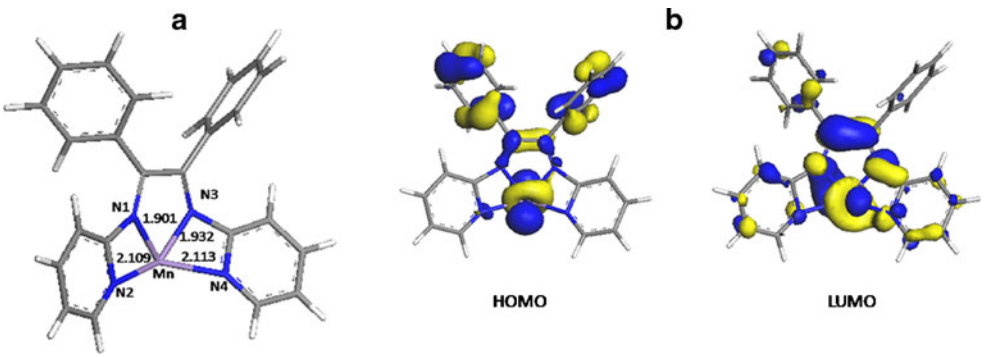

Fig. 6 DFT optimized structure of the Mn^{2+} complex of L (**a**) and HOMO and LUMO orbitals of the optimized complex

The number of Mn^{2+} ions bound to L and the binding constant (β) was determined in 1:1 (v/v) $CH_3CN:H_2O$ as reported [24–26] from the plot of $\log((F_o-F)/(F-F_{max}))$ versus $\log[Mn^{2+}]$ (Fig. 4). Where F_o is the fluorescence intensity of L in absence of Mn^{2+} ion, F is the fluorescence intensity of L at an added concentration of Mn^{2+} ion and F_{max} is the fluorescence intensity of L when concentration of Mn^{2+} ion attains fluorescence saturation. A least squares fitting of the data yielded a linear plot (R^2=0.9916) with slope 1.02 indicating that binding ratio between L and Mn^{2+} ion was 1:1, log β was found to be 3.05.

To confirm the number of Mn^{2+} ions bound to L and the binding constant, the UV/Visible spectra of L in 1:1 (v/v) $CH_3CN:H_2O$ (pH 4.0) at different added concentration of the Mn^{2+} ion was recorded (Fig. 5). L showed absorption maximum at λ_{max} value 360 nm. Upon addition of Mn^{2+} ions, the absorbance of the peak found to increase with a red shift from 360 nm to 370 nm. The plot of $\log((A_o-A_s)/(A_s-A_\infty))$ against $\log[Mn^{2+}]$ has been shown in Fig. 4, inset. Here, A_o, A_s and A_∞ are the absorbances of L when concentration of Mn^{2+} ion is zero, is an intermediate and at maximum absorbance value. A least squares fitting of the data yielded slope=1.25 (R^2=0.9919) confirming 1:1 binding between L and Mn^{2+} and log β value was calculated as 2.95 which is similar with that calculated from fluorescence data.

The binding between L and Mn^{2+} ion has been studied by DFT calculation. The optimized geometry of the manganese complex along with Mn-N distances are shown in Fig. 6. It is seen that the Mn-N bond distances are in agreement with available experimental results [27]. In the vibrational frequency calculations, no imaginary frequency was found for the complex suggesting that the optimized complex represents a stable structure (local minima) in the potential energy surface.

The enhancement in fluorescence intensity of L on interaction with Mn^{2+} ion may be explained on the basis of the thermodynamically favourable photo induced electron transfer (PET) mechanism between L and Mn^{2+}. From DFT calculation it is clear that Mn^{2+} ion binds to L via the four N-atoms of the pyridine moiety. In L the receptor part is the 2-amino pyridine and benzil is the fluorophore part (Scheme 1). In unbound L the PET process occurs due to the transfer of electron density, originating at the lone pairs of electrons on N atoms of the receptor moiety, to the LUMO of the fluorophore. Binding of Mn^{2+} to L through the lone pairs of N atoms hindered the PET process leading to fluorescence intensity enhancement.

In summary, we have presented a simple benzil and 2-amino pyridine based probe that could distinguish Mn^{2+} ion over Na^+, K^+, Ca^{2+}, Mg^{2+}, Ba^{2+}, Fe^{2+}, Co^{2+}, Ni^{2+}, Cu^{2+}, Zn^{2+}, Cd^{2+}, Hg^{2+}, Pb^{2+} and Ag^+ ions. The high selectivity for Mn^{2+} is marked by a significant fluorescent enhancement and a red shift in emission spectra. Spectroscopic data and DFT calculation has confirmed 1:1 binding between L and Mn^{2+} ion. The enhancement in fluorescence of L on binding Mn^{2+} ion is due to the photo induced electron transfer (PET) process.

Acknowledgment Department of Science & Technology, New Delhi and University Grants Commission (SAP), New Delhi are thanked for financial help.

References

1. Emsley J (2001) Nature's building blocks: An a-z guide to the elements. Oxford University Press, Oxford, pp 249–253
2. Law NA, Caudle MT, Pecoraro VL (1998) Manganese redox enzymes and model systems: properties, structures, and reactivity. Adv Inorg Chem 46:305–440
3. Dismukes GC, Willigen RTV (2006) Manganese: The oxygen-evolving complex & models. Encyclopedia of Inorganic Chemistry. Princeton University, Princeton
4. Takeda A (2003) Manganese action in brain function. Brain Res Rev 41:79–87
5. Bird ED, Anton AH, Bullock B (1984) The effect of manganese inhalation on basal ganglia dopamine concentrations in rhesus monkeys. Neurotoxicology 5:59–66
6. Gupta SK, Murthy RC, Chandra SV (1980) Neuromelanin in manganese-exposed primates. Toxicol Lett 6:17–20
7. Furst A (1978) Tumorigenic effect of an organomanganese compound on F344 rats and Swiss albino mice: brief communication. J Natl Cancer Inst 60:1171–1173
8. Young RJ, Critchley J, Young KK, Freebairn RC, Reynolds AP, Lolin YI (1996) Fatal acute hepatorenal failure following potassium permanganate ingestion. Hum Exp Toxicol 15:259–261
9. Bouchard MF, Sauve S, Barbeau B, Legrand M, Brodeur M, Bouffard T, Limoges E, Bellinger DC, Mergler D (2010) Intellectual impairment in school-age children. Environ Heal Perspect 119:138–143
10. Elsner RJF, Spangler JG (2005) Neurotoxicity of inhaled manganese: public health danger in the shower? Med Hypotheses 65:607–616
11. Cersosimo MG, Koller WC (2006) The diagnosis of manganese-induced parkinsonism. NeuroToxicology 27:340–346
12. Lu CS, Huang CC, Chu NS, Calne DB (1994) Levodopa failure in chronic manganism. Neurology 44:1600–1602
13. Lee HN, Xu ZC, Kim SK, Swamy KMK, Kim Y, Kim SJ, Yoon JY (2007) Pyrophosphate -selective fluorescent chemosensor at physiological pH: formation of a unique excimer upon addition of pyrophosphate. J Am Chem Soc 129:3828–3829
14. Wang JB, Qian XH (2006) Two regioisomeric and exclusively selective Hg(II) sensor molecules composed of a naphthalimide fluorophore and an o phenylenediamine derived triamide receptor. Chem Commun 109–111
15. Komatsu K, Urano Y, Kojima P, Nagano TJ (2007) Development of an iminocoumarin- based zinc sensor suitable for ratiometric fluorescence imaging of neuronal zinc. J Am Chem Soc 129:13447–13454
16. Goswami P, Das DK (2012) A new highly sensitive and selective fluorescent cadmium sensor. J Fluoresc 22:391–395
17. Goswami P, Das DK (2012) N, N, N, N-tetradentate macrocyclic ligand based selective fluorescent sensor for zinc (II). J Fluoresc 22:1081–1085
18. Zhang J, Campbell RE, Ting AY, Tisen RY (2002) Creating new fluorescent probes for cell biology. Nat Rev Mol Cell Biol 3:906–918
19. Shuhong X, Wang C, Zhang H, Sun Q, Wang Z, Cui Y (2012) Discriminative detection of bivalent Mn ions by a pH-adjustable

recognition method via quantum dot fluorescence sensing. J Mater Chem 22:9216–9221
20. Gruppi F, Liang J, Bartelle B, Royzen M, Turnbull DH, Canary JW (2012) Supramolecular metal displacement allows on-fluorescence analysis of manganese(II) in living cells. Chem Commun 48:10778–10780
21. Liang J, Canary JW (2010) Discrimination between hard metals with soft ligand donor atoms: an on fluorescence probe for Manganese (II). Angew Chem Int Ed 49:7710–7713
22. Haugland RP (2002) Molecular probes: Handbook of fluorescent probes and research products, 9th edn, Molecular Probes
23. Delly B (1990) An all–electron numerical method for solving the local density functional for polyatomic molecules. J Chem Phys 1990:508–514
24. Kulatilleke CP, Silva SA, Eliav Y (2006) A coumarin based fluorescent photoinduced electron transfer cation sensor. Polyhedron 25:2593–2596
25. Goswami P, Baruah S, Das DK (2010) 2,7-Dichlorofluorescein, a fluorescent sensor to detect Cd^{2+} over Na^{+}, K^{+}, Ca^{2+}, Cu^{2+}, Ni^{2+} and Zn^{2+}. Indian J Chem 49A:1617–1620
26. Dutta K, Das DK (2012) 2,7-Diferrocenyl-3,6-diazaocta-2,6-diene: a highly selective dual fluorescent sensor for Zn^{2+} and Ag^{+} and electrochemical sensor for Zn^{2+}. Indian J Chem 51A:816–820
27. Baca SG, Siminov YA, Gerbeleu NV, Gdaniec M, Bourosh PN, Timco GA (2001) Synthesis and X-ray diffraction study of Zn(II) complexes with o-phthalic and aromatic amines. Polyhedron 20:831